The Journal of Adhesion, 83:705–722, 2007
Copyright © Taylor & Francis Group, LLC
ISSN: 0021-8464 print/1545-5823 online
DOI: 10.1080/00218460701490363

Friction and Adhesion Hysteresis between Surfactant Monolayers in Water

Wuge H. Briscoe
Physical and Theoretical Chemistry Laboratory, University of Oxford, Oxford, United Kingdom

Jacob Klein
Physical and Theoretical Chemistry Laboratory, University of Oxford, Oxford, United Kingdom and Department of Materials and Interfaces, Weizmann Institute of Science, Rehovot, Israel

We briefly review the model that correlates friction between two surfaces in adhesive contact with the loading–unloading adhesion hysteresis between them. We then examine in light of this model the observed low friction between two mica surfaces coated with a double-chained quaternary ammonium surfactant in intimate adhesive contact in water. This enables us to propose a mechanism for surfactant boundary lubrication in water that is rather different from the classic boundary lubrication in air: in this mechanism, adhesion takes place at the interface between the opposing surfactant hydrocarbon tails, whereas frictional sliding takes place at the interface between the hydrated surfactant headgroups and mica. The implications of our findings to biolubrication processes are discussed.

Keywords: Adhesion hysteresis; Aqueous boundary lubrication; Biolubrication; Friction under water; Hydration layers; Slip-plane shift; Surface forces; Surfactant monolayers

INTRODUCTION

With the rapid advent of nanotechnology, the surface-to-volume ratio in devices and in nanostructured materials grows, and with it the

Received 18 February 2007; in final form 16 May 2007.

One of a Collection of papers honoring Liliane Léger, the recipient in February 2007 of *The Adhesion Society Award for Excellence in Adhesion Science, Sponsored by 3M.*

Wuge Briscoe is visiting scientist at Fakulteten för teknik-och naturvetenskap, Karlstad University, Universitetsgatan 1, SE65188 Karlstad, Sweden.

Address correspondence to Jacob Klein, Physical and Theoretical Chemistry Laboratory, University of Oxford, South Parks Road, Oxford OX1 3QZ, UK. E-mail: jacob.klien@chem.ox.ac.uk

importance of surface interactions. For instance, in microelectromechanical systems (MEMS) [1,2], it is important to control adhesion, friction, and wear of minute mechanical components to ensure their performance and durability. An effective strategy for this is to attach monolayers of hydrocarbons (or fluorocarbons) on the solid surfaces. This may be done covalently for suitable solid surfaces with thiols and silanes [3–5]. Alternatively, in an aqueous medium, surfactant or lipid molecules may be self-assembled onto the solid surface [6,7] or *via* Langmuir–Blodgett (LB) deposition [3]. Such surfactant layers lead to so-called boundary lubrication, where rubbing between the underlying substrates is largely replaced by sliding between the surfactant layers, coating them at their boundaries, either in air or oil media [8,9]. The efficiency of this process is thought to result from the weak shear stresses needed to slide the boundary layers past each other, thereby resulting in friction coefficients that are lower than those between the underlying solid substrates. At the same time as some reduction in the friction [10,11], boundary lubrication, by largely preventing substrate–substrate scuffing, often results in massive reduction in wear [8,9].

As demonstrated by experimental [10,12], theoretical [13,14], and computer simulation [15] studies, the van der Waals bonds at the interface between the surfactant layers (in organic media, including oil, or in air) are the weakest link with respect to shear, so slip takes place here rather than at the solid–surfactant interface. Then the shear characteristics and lubrication effectiveness are predominantly determined by the properties of the surfactant tails, such as the chain length, the packing density of the monolayer, the molecular architecture of the surfactant, as well as external parameters such as temperature, applied load, and the humidity of the surrounding environment [4,11]. It is of interest that frictional or shear stresses, σ (sliding friction force normalised by the interacting surface area; $\sigma = F_s/A$), mediated by surfactant monolayers [10,11,16], typically ranging between 0.1 MPa and a few MPa, are comparable with those mediated by simple hydrocarbon liquids [17,18].

Surfactant molecules are also ubiquitous in aqueous media and may adsorb readily onto solid surfaces. How would they participate in the tribological process in aqueous media? Such a question is relevant to nanofluidics and MEMS and to the understanding of the biolubrication process in which phospholipids have been implicated [19,20]. However, few systematic studies on boundary lubrication by surfactants immersed in aqueous media have been carried out [21–26]. Using a mica surface force balance [27,28], we have measured friction between two mica surfaces bearing self-assembled double-chain cationic surfactant in intimate, strongly adhesive contact immersed in pure water. A striking feature of our observation is that the measured frictional stress in water is substantially lower—by some 90–99%—than the typical values reported in boundary lubrication in air or oil. This was ascribed to the shift of the slipplane from the midlayer interface to the surfactant–headgroups/mica interface, where the hydration layer surrounding the headgroups provided better lubrication and so became the weakest link. At the same time, it was postulated that the adhesion plane—the interface where the surfaces adhered and separated—remained at the midplane between the surfactant layers. Here we examine in more detail (following the earlier brief report [29]) this unexpected separation of plane of adhesion and plane of friction in the light of a model [11] whose validity has been reasonably well established for classic boundary lubrication (where adhesion and slip both occur at the midplane between the surfactant layers).

FRICTION AND ADHESION HYSTERESIS

In contrast to the intuitive sense that friction between two sliding surfaces should be correlated with the strength of the adhesion between them, Israelachvili and coworkers have suggested that in certain circumstances it is rather the adhesion *hysteresis* (as explained later) that is correlated with the friction (see, *e.g.*, Ref. 11). This suggestion was based on studies of friction, adhesion, and adhesion hysteresis between monolayer-coated surfaces across a spectrum of surfactants and simple hydrocarbon liquids in adhesive contact over a wide range of conditions. The basic model is illustrated schematically in Figure 1.

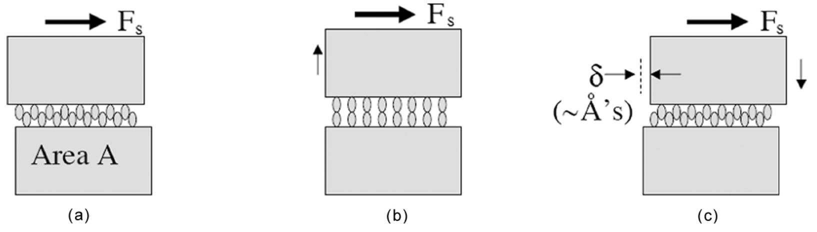

FIGURE 1 Schematic of the model relating adhesion hysteresis to friction between sliding surfaces across an area A: As the force F_s required to overcome friction moves the top surface, it detaches by a microscopic amount as shown in b, which costs some surface energy γ_1. (The protrusions shown can be surfactant ends or even atomic corrugations.) On further motion, the surfaces readhere at c (displaced laterally by a microscopic distance δ from a), regaining a surface energy, γ_2. The net energy loss is $|(\gamma_1 - \gamma_2)|A = A\Delta\gamma$, which correlates with the frictional work done, $F_s\delta$, so that $F_s/A \approx \Delta\gamma/\delta$.

Here two surfaces coated with a lubricating layer and in adhesive contact over an area A, Figure 1a, are made to slide past each other. The friction force required to slide them is F_s. As they slide, there is assumed to be some microscopic vertical displacement, as indicated in Figure 1b, which is recovered on further sliding. Such microscopic vertical displacement may arise when bonds are sheared on sliding on a microscopically rough surface (even perfectly smooth single-crystal surfaces have atomic or subatomic scale asperities) or when interdigitated surfactant layers slide past each other. When the surfaces come together again after some microscopic lateral displacement δ (of order Ångströms (Å's)), as indicated in Figure 1c, some energy may have been irreversibly lost because of the cycle of adhesive bond breaking (Figure 1a to Figure 1b) and reforming (Figure 1b to Figure 1c). We suppose this energy loss (per unit area) to be similar to the difference in surface energy, $\Delta\gamma$, arising from breaking and reforming the adhesive junction between the surfaces in a separation–readherence cycle (so-called adhesion hysteresis). Finally, we equate the resulting energy loss over the area of contact of the surfaces, $A\ \Delta\gamma$, to the energy dissipation arising from the work done by the frictional force, F_s, in moving laterally by δ, which is just $F_s\delta$. Thus, we obtain the relation

$$A\ \Delta\gamma \approx F_s\delta,$$

or

$$\frac{F_s}{A} \approx \frac{\Delta\gamma}{\delta}. \tag{1}$$

This is the central result [11] relating the adhesion hysteresis, $\Delta\gamma$, to the frictional stress, $\sigma = F_s/A$, and gives an order of magnitude estimate of the frictional or shear stress directly from $\Delta\gamma$ (given that the shear velocity is comparable with the loading–unloading velocity). Good agreements have been found between Eq. (1) and the measured shear stress between adsorbed surfactant layers over a range of different surfactants in dry and humid conditions, and in organic vapours (*e.g.*, Ref. 11), suggesting that the correlation applies reasonably well in such conditions.

The actual magnitude of the adhesion hysteresis may be extracted from loading/unloading experiments between two curved surfaces, *via* the contact mechanics relation that connects the contact area, A, between them under a compressive load with the surface energy, γ. The Johnson–Kendall–Roberts (JKR) theory of contact mechanics [30] relates A to the applied load, L, for surfaces of initial undeformed radius, R, and the bulk modulus, K, of the substrates,

$$A = \pi\left\{\left(\frac{R}{K}\right)\left[\mathrm{L} + 6\pi R\gamma + \left(12\pi R\gamma L + (6\pi R\gamma)^2\right)^{1/2}\right]\right\}^{2/3}. \tag{2}$$

Because the only unknown in this relation is the surface energy, γ, it may be extracted by fitting the loading curves, which yield a surface energy, γ_{L}, and the unloading curves, which yield a surface energy, γ_{U}. The adhesion hysteresis is then given by the difference, $\Delta\gamma = |(\gamma_L - \gamma_L)|$.

EXPERIMENTAL SECTION

Our measurements are performed between two mica surfaces of micrometer thickness bearing the double-chained cationic surfactant, N,N-dimethyl-N,N-diundecylammonium bromide $[(CH_3(CH_2)_{10})_2 N^+(CH_3)_2Br^-]$, kindly provided by R. K. Thomas and D. J. McGillivray, using a surface force balance (SFB) [27,31], which enables both shear and normal forces between the surfaces to be determined directly. The surfactant is first dissolved in water [purified with a RiOs5$^{\mathrm{TM}}$-MilliQ$^{\mathrm{TM}}$ Gradient A10 system (UK); resistivity $> 18.2\ \Omega\cdot$cm and total organic content ≤ 4 ppb] in 0.3–3 mM concentration ($\sim$10–100 CMC) at $\sim$25°C and then adsorbs onto the immersed mica surfaces *via* both ion exchange with K^+ desorbing from mica and a physisorption mechanism. The mica surfaces of 1–2 cm^2 in size and 1–3 μm in thickness were freshly cleaved and coated with $\sim$50-nm silver on one side. They are then glued onto cylindrical silica lenses of radius $R \sim 1$ cm using an epoxy resin (Epon 1004, Shell®, Danbury, Connecticut, USA). The immersion time of mica in the surfactant solution for the results presented here is 10 min (though other measurements, not shown, were carried out also for a range of other immersion times). After withdrawal from the surfactant solution, the surfaces are rinsed thoroughly with water and dried in a small stainless steel desiccator in the presence of P_2O_5 (98%+, Aldrich®, UK) for $\sim$15 h before being mounted in the SFB.

In an SFB, the normal forces, F_{n}, and lateral (shear or friction) forces, F_{s}, between the surfaces can be measured simultaneously as a function of surface separation, D, by monitoring the deflections of two springs onto which the surfaces are mounted, as schematically shown in Figure 2. The top surface is made to move parallel to the bottom surface at a constant shear velocity, V, by bending a hollow piezoceramic (PZT) cylinder. (The implementation of the lateral spring is described in detail in Ref. 27.) Such an implementation affords a sensitivity of better than 0.2 μN in friction detection and is well suited to

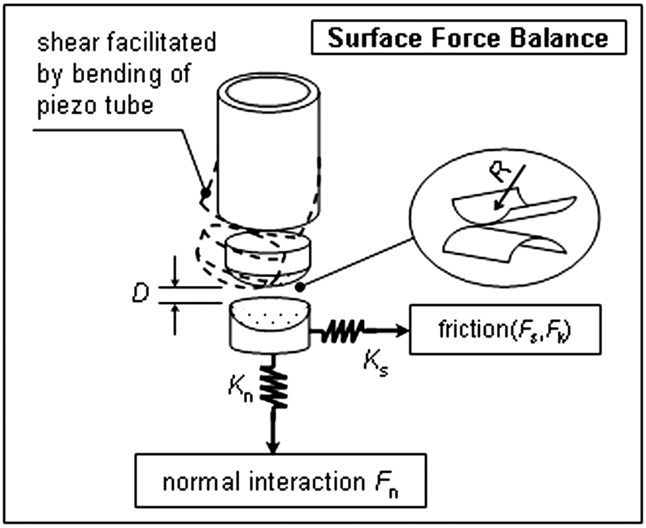

FIGURE 2 Schematic of the surface force balance (SFB) [27], in which the normal, F_n, and lateral, F_s, interactions between two crossed cylindrical mica surfaces can be measured simultaneously as a function of separation, D, by monitoring the deflections of two springs of force constants, K_n and K_s, respectively. The radius, R, of the surfaces is typically $\sim 1\,\mathrm{cm}$, and the interacting area between the surfaces when they are in contact can be estimated using the Hertz theory or the Johnson–Kendall–Roberts (JKR) theory of contact mechanics, respectively, for the nonadhesive and adhesive contacts [30] or can be measured from the shape of the optical fringes when the surfaces are in contact. Thus, the shear stress (friction normalized by the contact area) can be obtained. (The SFB is described in detail in Ref. 27.)

measure low friction that is inaccessible with alternative designs. All the measurements described here are carried out at $25 \pm 0.5^\circ\mathrm{C}$. The SFB used in this study was constructed by the workshops at the authors' department at Oxford University.

RESULTS

Surfactant-coated surfaces experience strong adhesion both in dry air (in the presence of P_2O_5) and in water. In air, the pull-off force, F_p, to separate the surfaces from the adhesive contact, $F_p/R = -277 \pm 33\,\mathrm{mN/m}$, gives, within the JKR theory of contact mechanics [30], a surface energy $\gamma = -(F_p/R)/(3\pi) = 29.3 \pm 4\,\mathrm{mJ/m^2}$. This value is within the range of literature values of 22–28 $\mathrm{mJ/m^2}$ [32], though it appears slightly higher. The small difference may be ascribed to the presence of surface defects that allow the hydrocarbon tails to interdigitate. The total surfactant layer thickness is $D_0 = 2.7 \pm 0.4\,\text{nm}$, smaller than twice the total molecular length of the surfactant, 3.8 nm, indicating that the molecules adsorb onto the mica surface with the hydrocarbon tails tilted.

When water is introduced between the surfaces and they are allowed to approach each other *for the first time* within a few minutes after the water introduction, the surfaces spontaneously jump from around $D_j = 15$–$20\,\text{nm}$ into an adhesive contact. The adhesion is now markedly stronger between two surfaces than in air, with $F_p/R = -358.4 \pm 66\,\text{mN/m}$ and $\gamma = 40 \pm 6\,\text{mJ/m}^2$, whereas the total surfactant thickness is slightly higher than in air with a swelling of $\Delta D_0 \sim 0.5\,\text{nm}$ (a mean value based on several experiments, including those where longer incubation times were used for the surfactant coating with a scatter of $\sim 0.4\,\text{nm}$). This is attributed to the development of a hydration layer around the quaternary surfactant headgroup at the mica surface. If the surfaces are separated (after friction measurements at this virgin contact) and brought into contact again at the same point, we find the pull-off force becomes somewhat smaller, $F_p/R = -280 \pm 38\,\text{mN/m}$ and $\gamma = 29.6 \pm 4\,\text{mJ/m}^2$, whereas swelling similar to that at the virgin contact is preserved.

Under the strong adhesion that the surfaces experience in their virgin contact (in both air and water as described previously), they become elastically deformed to form a flattened contact region between them. This region is approximately circular in shape and has an area, A, of the order of $1000\,\mu\text{m}^2$. It is over this flattened, strong adhesive contact that we measure the kinetic friction force, F_k, between the surfaces, and the results are reported in Figures 3 and 4.

Figure 3A shows a sawtooth trace of the applied shear motion as a function of time, the slope of which gives the shear velocity V. As shown in Figure 3B, the friction *vs.* time trace in air exactly tracks the applied shear, indicating that the surfaces remain rigidly coupled to each other in air for all the applied shear amplitudes, Δx_0 (10–1800 nm) and shear velocities, V (2–5000 nm/s). Therefore, friction between two surfaces must exceed the maximum applied shear force, $K_s \Delta x_{0,\text{max}}/2$, where $\Delta x_{0,\text{max}}$ is the maximal applied lateral motion (peak to peak value in Figure 3A). We find $K_s \Delta x_{0,\text{max}}/2 > 220$–$250\,\mu\text{N}$, corresponding to the upper hatched region in Figure 4. Given that friction (F_k) varies with the true contact area (A) between the surfaces [9], it is appropriate to compare our results with those in the literature in terms of shear stress, $\sigma(=F_k/A)$, between the surfaces. In our case, $A \sim 1000\,\mu\text{m}^2$, and thus rigid coupling in air implies that σ between the surfaces in air is greater than $\sim 0.1\,\text{MPa}$. In fact,

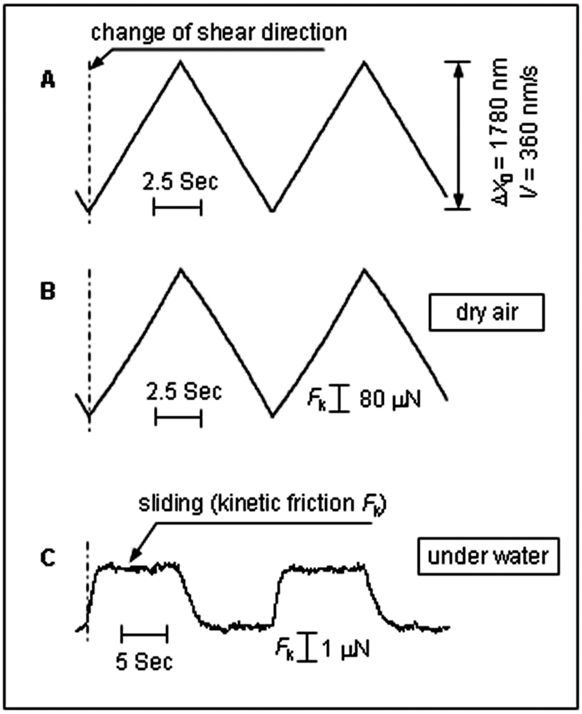

FIGURE 3 Applied shear motion and typical friction force traces between two surfactant-coated surfaces. Trace A shows the sawtooth-shaped shear motion applied to the top surface when friction measurements are carried out. The shear response between two surfactant-coated surfaces in dry air (trace B) has a sawtooth shape identical to the applied shear, indicating that surfaces remain rigidly coupled to each other. Trace C, taken from a different experiment, illustrates the shear force when two surfaces are in their virgin adhesive contact in pure water. (The slight asymmetry in the slopes arises from a small nonlinearity in the PZT response at high amplitudes.) Note that the friction force scales in B and C differ by a factor of 80 (adapted from Ref. 29).

previous boundary lubrication studies have reported values for shear stress between surfactant-coated surfaces in air in the range of 0.1–4 MN/m^2 or higher [10,11,33,34], comparable with, or well more than the maximum shear stress that we applied in air.

If water is introduced between the surfactant-coated surfaces, the adhesion between the surfaces in intimate contact is bigger, yet the friction between them is then reduced very substantially. A typical shear force *vs*. time trace is shown in Figure 3C, and the plateau regions correspond to smooth sliding between the surfaces. The

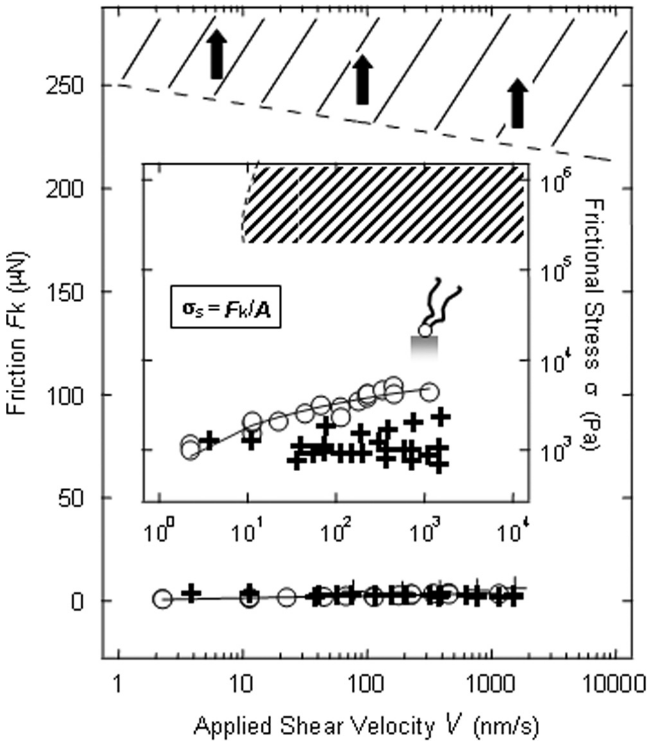

FIGURE 4 Main figure shows the velocity (V) dependence of measured kinetic friction (F_k) on a linear–log scale, and the inset shows that for shear stress (σ_s) on a log–log scale. The hatched regions in the figure indicate the friction and shear stress values for classic boundary lubrication in air. The circles (O) are friction stresses collected from the experiments in which the surfactant-coated surfaces are kept separated during water injection, whereas the crosses (+) form the experiments in which the surfaces remained in contact during water injection. The solid curves are a guide to eyes (adapted from Ref. 29).

measured friction, taken from the sliding sections of the friction trace, is mildly velocity dependent as shown in the main figure and the inset (open circles ○) in Figure 4, increasing slightly with V. [The data shown in crosses (+) are collected using a different experimental procedure as described in detail in the Discussion section.] The velocity dependence may be fitted with a logarithmic curve, *i.e.*, $F_k \sim \ln(V)$, but a power law could be fitted equally well. The solid curves in Figure 4 are a guide for the eye.

As shown in Figure 4, the most remarkable feature of our observations is the striking reduction in the magnitude of the friction force (main figure) or shear stress (inset) between the surfaces in water relative to air. The values in water lie in the range of 0.001–0.01 MPa, two to three orders of magnitude lower than the literature values (or our own measurements in dry air, main Figure 4) for shear stress from boundary lubrication studies in air, which is shown as the hatched area [10,11,33,34] in the inset.

To get further insight into the origins of this large reduction in the friction, we carried out loading–unloading cycles (increasing or decreasing loads, L) for the surfactant-coated surfaces while monitoring the contact area, A, both in air and in water, and compared the observed adhesion hysteresis. Figures 5A and 5B show the A *vs.* L curves obtained, respectively, in air and in water (at the virgin contact). Using $K = 10^{10}\,\mathrm{N/m^2}$ [27] and fitting the curves to Eq. (2) yields $\Delta\gamma \approx 20 \pm 2\,\mathrm{mJ/m^2}$ both in dry air and under water. Thus, using the relation from the adhesion hysteresis model, $\sigma \sim \Delta\gamma/\delta$, and with $\delta \sim 0.5$–$1\,\mathrm{nm}$, we obtain $\sigma \approx (2-4) \times 10^7\,\mathrm{N/m^2}$. Though this value is within the range of the shear stress in dry air as reported in some previous studies, it is some orders of magnitude too high compared with the values that we have measured, *i.e.*, 1 to $10 \times 10^3\,\mathrm{N/m^2}$.

DISCUSSION

Our system, where two solids coated with surfactant monolayers rub against each other, is reminiscent of classical boundary lubrication. In boundary lubrication, the interacting surfaces are often the nonpolar chains, and thus, the friction is largely determined by the properties of these chains (their packing, fluidity, and density) and parameters that can affect these properties such as temperature and chain length. These are the same properties that affect adhesion (and adhesion hysteresis, $\Delta\gamma$), a similarity which underpins Eq. (1) relating the friction to $\Delta\gamma$. Applying Eq. (1) to our system results in a consistent picture for dry air, but in water the same equation predicts a friction that is too high by some orders of magnitude.

What is the reason for this discrepancy and for the very low friction under water? One clue is provided by the slight swelling, $\Delta D_0 \sim 0.5\,\mathrm{nm}$, that we have observed following immersion of the surfactant-coated surfaces in water. This is likely due to uptake of water by the quaternary ammonium ions (*i.e.*, the headgroups of the DunDAB surfactant used). Much effort has been made to understand the hydration properties of such ions [35,36]. Although the exact number of water molecules that bind to quaternary ammonium ions is reported to range

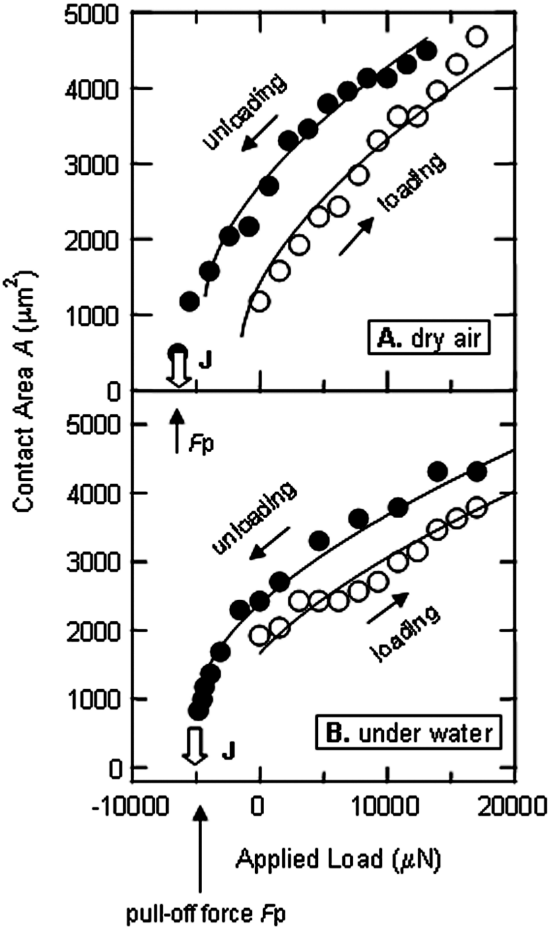

FIGURE 5 Loading–unloading profiles of surfactant-coated surfaces showing variation of contact area, A, with load, L: A) in dry air and B) under water at the virgin contact. The solid curves are fits to the JKR theory [Eq. (2) in text]; in both cases the adhesion hysteresis $\Delta\gamma \sim 20\,\text{mJ/m}^2$ (adapted from Ref. 29).

from 2 to 16 [35,37,38], it is clear that they have a strong affinity for water uptake, and the swelling, ΔD_0, suggests that water penetrates into the surfactant layer and hydrates the headgroups located at the hydrophilic mica surface [39]. The extent of swelling is particularly suggestive: $\Delta D_0 \sim 0.5\,\text{nm}$ is close to twice the swelling of surfactant monolayers (0.25 nm each) with similar cationic ammonium headgroups, intercalated in vermiculite clays, measured by neutron diffraction [40], when taken from the dry to the wet state. In practice, there is reason to believe that the real swelling of each headgroup layer due to its hydration is somewhat larger than $\Delta D_0/2$: this is because it is likely that, upon hydration, the mean *lateral* spacing of the headgroups on the mica surface also increases [11], so that the hydrophobic tail layer shrinks somewhat, by δh say. The net dilation $(\Delta D_0/2)$ in the overall layer thickness then represents this shrinkage, δh, compensated by a swelling of the actual headgroup layer by an amount $[(\Delta D_0/2) + \delta h]$.

It is known that the lateral mobility of surfactant headgroups attached to a surface may be enhanced at higher humidities [41,42]. This may be related to the observed very high fluidity of surface-bound ions in shear [43], ascribed to the high exchange rate of water molecules in the bound hydration layer with those either in bulk water or from other (adjacent) hydration shells. It is known that such fluidity massively reduces the friction between two (charged) rubbing surfaces across an aqueous salt solution [43,44]. Thus, we may attribute the substantial reduction in friction upon immersion in water to the hydration of the charged headgroup layer at the mica interface and to its consequent fluidity with respect to shear of that interface. That is, we believe that sliding occurs not at the midplane between the surfactant layers as in classical boundary lubrication, but at the headgroup–mica interface.

How can we reconcile this with the adhesion hysteresis results, which show that both the magnitude of the adhesion (as revealed by the pull-off forces) and that of $\Delta\gamma$ are rather similar whether in dry air or under water? This similarity indicates that the interface at which the two surfactant layers separate on being pulled apart, and re-adhere on approach, is the same: because we know that in dry air this interface is the midplane one between the alkyl tail layers, this then must also be the case when immersed in water. That is, the plane of adhering and de-adhering lies at the interface between the hydrocarbon tails, whereas upon shear, sliding takes place at the mica–headgroup interface: this is because, following its hydration, that interface becomes the plane of least resistance to shear. This contrasts with the usual boundary lubrication scenario where both the slip plane and the adhesion plane are between the alkyl tail layers.

To examine whether this is reasonable from an energetic point of view, we may estimate the adhesive forces at the different interfaces. In the following, we assume the monolayers detach intact on pull-off so that surfactant molecules remain within their layers when the layers come apart (*i.e.*, we do not pull individual surfactants out of their layer). The hydrophobic adhesive force, $f_{\mathrm{surf/surf}}$, per surfactant molecule at the surfactant–surfactant interface may be written as $f_{\mathrm{midplane}} = -[\partial E/\partial D]_{D=0}$, where the hydrophobic energy (per surfactant molecule) $E \approx -(\gamma s^2)e_0^{-D/h}$; here γ is the interfacial energy at the hydrophobic tail/water interface $\approx 35 \pm 5\,\mathrm{mJ/m^2}$ (from the pull-off forces), $s^2 \approx 50$ Å^2 is the mean area per surfactant molecule, and $h_0 \approx 1\,\mathrm{nm}$ is the decay length for the hydrophobic attraction. This yields $f_{\mathrm{surf/surf}} = -(\gamma s^2)/h_0 \approx -(2 \pm 0.3) \times 10^{-11}\,\mathrm{N}$. The adhesive force, $f_{\mathrm{surf/substrate}}$, per surfactant molecule attached by a positively charged polar head at the negatively charged substrate may be estimated as $f_{\mathrm{surf/substrate}} = -e^2/(4\pi\varepsilon\varepsilon_0 x^2)$, where $x \approx 4$ Å is the charge separation and e is the electronic charge. The effective dielectric constant for layers of water comparable in thickness, l, with a hydration layer is much less than that of the bulk and has been both calculated [45] and evaluated from experiment [46] as $\varepsilon \approx 5$–10 for $l < 1\,\mathrm{nm}$. This gives $f_{\mathrm{surf/substrate}} \approx -(1-2) \times 10^{-10}\,\mathrm{N}$, an order of magnitude or so larger than $f_{\mathrm{surf/surf}}$. This estimation assumes that the hydration layers detach with the polar headgroups to be replaced by water at the mica surface. The conclusion is that pull-off upon separation indeed occurs at the interface between the hydrocarbon tails, even though sliding occurs at the headgroup–substrate interface, in line with our earlier suggestion.

Other aspects of our findings and interpretation need further consideration. One could ask how dry our monolayers are in the "dry air" in the presence of P_2O_5 in the drying chamber, so that our proposed mechanism of hydration under water is still valid (*i.e.*, would the headgroups, which were deposited from aqueous solution and so presumably hydrated when deposited, not retain their hydration layers even in dry air?). This can be addressed from two viewpoints. Firstly, the swelling ($\Delta D_0/2$) of each layer measured in our force experiments, by an extent close to that measured independently by neutron scattering for monolayers of surfactants with similar headgroups [40], strongly suggests that our monolayers are indeed largely dry prior to adding water. Moreover, such drying-out of the hydration layers in surfactant monolayers, or of highly confined hydrated ions, in the conditions of our experiments is known from earlier studies on dehydration of surfactant headgroups. For example, in Ref. 40 the hydration of similar surfactant headgroups could be readily reduced by maintaining them in a desiccator at room temperature even when the surfactants were intercalated in pores of vermiculite clay, whereas, in an earlier study, Keren and Shainberg [47] could reversibly control the degree of hydration of $\mathrm{Na^+}$ ions confined in montmorillonite clays by exposure to different levels of water vapour. Second, this ready equilibration of the water in surfactant layers is consistent also with NMR studies showing that most of the water hydrating the surfactant headgroups in soap–water mesophases has bulk-like mobility [48]. It is also in line with the work showing a bulk-like water structure and rotational mobility for water confined to lamellar films as thin as 1 nm [49]. These studies show that water in such surfactant layers is very mobile, and a substantial drying-out of our surfactant monolayers is indeed likely to occur readily when exposed to a dry atmosphere in the presence of P_2O_5 in our force balance.

A further issue is that sliding at the surface would lead to possible "pile-up" of excess surfactant molecules just outside the contact zone. However, a recent study [50] shows that the healing of the surfactant layers is very rapid, on some millisecond timescale. Thus, it is possible that the piled-up surfactant molecules may rearrange on the surface, so that healing occurs on the timescale of the shear motion. An interesting scenario, however, is that the ease (*i.e.*, low friction) of moving the surfactant molecules laterally suggests an alternative path to remove surfactant or lipid molecules from a substrate: rather than pulling them off, one could shear them off. One notable example could be found in the mechanism of recurrent epithelial erosion, in which persistent epithelial defects form over the cornea, and the newly formed epithelium can be easily detached by shear effected by the eyelid motion. Holly [51] has ascribed the mechanism to the reduced "adhesiveness" of the corneal epithelium to the underlying basement lipid membrane and the tissue (called storma) when the basement membrane becomes hydrated. In the light of our proposed lubrication mechanism, it is possible that the epithelium is not detached by pulling off; rather, the enhanced mobility could lead it to being sheared off—it is, thus, a frictional failure rather than an adhesive failure.

There is finally the question of whether the lower friction that we observe when immersing our surfaces in water might be due, in part, to a long-known process [52–55] termed "flip-flop" or "overturning," in which the surfactant molecules overturn so that their headgroups appear at the surfactant–water interface, as illustrated schematically in Figure 6A. The headgroups of such flip-flopped molecules would become hydrated (Figure 6A), and their hydration shells might then provide lubrication so that slip (or some slip) occurs at the midplane, rather than exclusively at the headgroup–substrate interface as we postulate.[1] To examine this, we carried out measurements [29] in which the two surfactant-coated surfaces were brought into contact *while in dry air*, water was added, and the friction forces were

---

[1] This possible flip-flop of surfactant molecules, stimulated by shear and prolonged exposure to water, could also contribute to the observed reduced adhesion energy upon contacts subsequent to the virgin contact we have observed.

measured without separation. The situation is then as shown schematically in Figure 6B, where there is no opportunity for flip-flop to occur (as there is no water available for headgroup hydration between the hydrophobic tail layers) and contact is presumably between the tails alone. In these measurements, we observed first that even though the surfaces were adhered when the water was added, a swelling, ΔD_0, occurred whose magnitude ($\sim 0.5\,\mathrm{nm}$) was very similar to that observed when water was added to the separated surfaces in the earlier configuration. Second, the sliding friction forces (or frictional stresses), indicated by crosses in Figure 4, were just as low, or even lower than, for the usual configuration where water is added while the surfaces are held apart (open circles in Figure 4). Because this low friction occurs for a situation with no overturned surfactant molecules, we conclude that the mechanism we postulated is indeed correct—that slip occurs at the substrate rather than at the midplane. It is interesting to speculate that the slightly higher frictional stress for the case of layers that had been exposed to water prior to contact relative to those that had not been so exposed (open circles *vs*. crosses in Figure 4 inset) may indeed arise from a small number of overturned molecules. This is because any unhydrated tails of the flip-flopped surfactant molecules in contact with the substrate—as in Figure 6A—would experience a higher friction when the surfactant layer slides past the mica.

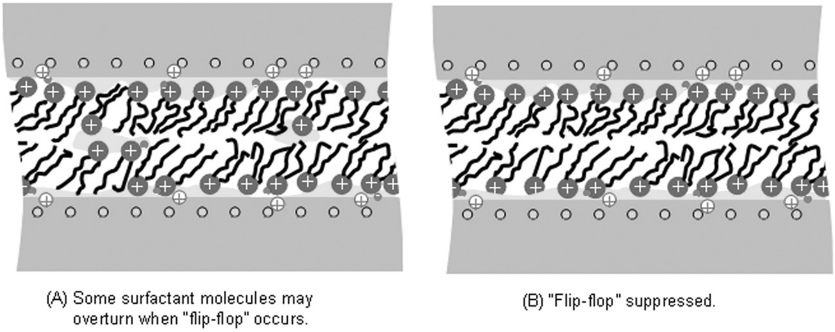
(A) Some surfactant molecules may overturn when "flip-flop" occurs.

(B) "Flip-flop" suppressed.

FIGURE 6 A) Molecules in a surfactant layer may overturn when in contact with water and become hydrated, so friction between two such layers may be facilitated by the hydrated headgroups at their midplane. B) When the surfaces are made to adhere prior to introducing water, overturning of molecules is suppressed, so that hydration can occur only at the headgroup–substrate interface.

The possible lubrication behaviour of hydrated groups may have some interesting implications for designing lubricants for aqueous media. Thus, surfactant molecules and water-soluble macromolecules, particularly polyelectrolytes [44], may be anchored onto the surface to modify the surface properties to facilitate desirable lubrication properties. In addition, many biological tissue surfaces—such as articular cartilage [56] and the eyelid past the cornea [57]—are known to slide past each other with considerable ease. These surfaces invariably bear phospholipids and macromolecules such as proteoglycans and polysaccharides, and the functions of those molecular components of the tissue surface in the biolubrication process are still under active debate. There have been suggestions that surface active phospholipids take part in biolubrication in a fashion analogous to boundary lubrication such that the hydrocarbon tails of the lipids glide over each other [19,20]. However, the actual friction coefficients observed in biological systems are very much lower than in classical boundary lubrication where tail–tail sliding occurs [9]. We suggest, therefore, that if phospholipids are indeed implicated in such lubrication, it is their hydrated headgroups rather than their tails that facilitate the highly efficient lubrication process. Indeed, the realization of the effectiveness of hydration layers in reducing friction between rubbing surfaces could offer a unifying view to underpin the extremely efficient lubrication in biological systems. This follows because all the biomolecules and biomacromolecules that have been implicated in biolubrication bear charged groups [20,56]: it may be that those hydrated charged groups are the important basic element in the lubrication rather than the molecule that carries them.

CONCLUSIONS

In conclusion, using a surface force balance, we have observed that frictional stress between mica surfaces coated with a dichain surfactant monolayer is reduced markedly in pure water compared with in dry air, by up to two orders of magnitude, although the adhesion hystereses are comparable in both cases. We ascribe this to the separation of the planes of adhesion and slip when under water. The former is located at the interface between the hydrocarbon tails, just like in air, giving rise to the large adhesion hysteresis comparable in air. The plane of slip when sliding occurs under water, however, is found to shift to the interface between the hydrated headgroups and the mica substrate, where the high fluidity of the hydration sheath around the headgroups results in the observed greatly reduced friction.

ACKNOWLEDGMENTS

We thank Simon Titmuss, Robert Thomas, Fredrik Tiberg, Duncan McGillivary, Stephen Garroff, Susan Perkin, Meng Chen, Neale Harvey, and Jacob Israelachvili for helpful discussions and the Mechanical and Electronic Workshops at the Physical and Theoretical Chemistry Laboratory, Oxford University, for their technical assistance. Ivan Vakarelski kindly sent W. H. B. a copy of Ref. 21. The surfactant used in this study was kindly provided by the Thomas Group at Oxford University. Financial support from Engineering and Physical Science Research Council (UK), the Petroleum Research Fund (American Chemical Society, Grant No. 45694-AC7), the Israel Science Foundation, and the McCutchen Foundation is gratefully acknowledged. W. H. B. also thanks Wolfson College, Oxford University, for a Junior Research Fellowship.

REFERENCES

[1] Singer, I. L., *J. Vac. Sci. Technol. A* **12**, 2605–2616 (1994), and references therein.
[2] Maboudian, R., *MRS Bulletin* **23**, 47–51 (1998), and references therein.
[3] Ulman, A., *An Introduction to Ultrathin Organic Films: From Langmuir–Blodgett to Self-Assembly* (Academic Press, Boston, 1991).
[4] Zhang, Q. and Archer, L. A., *J. Phys. Chem. B* **107**, 13123–13132 (2003).
[5] Kim, S., Christenson, H. K., and Curry, J. E., *Langmuir* **18**, 2125–2129 (2002).
[6] Clark, S. C. and Ducker, W. A., *J. Phys. Chem. B* **107**, 9011–9021 (2003).
[7] Fujii, M., Li, B. Y., Fukada, K., Kato, T., and Seimiya, T., *Langmuir* **17**, 1138–1142 (2001).
[8] Hardy, W. and Bircumshaw, I., *Proc. R. Soc. Lond. A.* **108**, 1–25 (1925).
[9] Bowden, F. P. and Tabor, D., *The Friction and Lubrication of Solids* (Oxford University Press, Oxford, 1950).
[10] Briscoe, B. J. and Evans, D. C. B., *Proc. R. Soc. Lond. A.* **380**, 389–407 (1982).
[11] Yoshizawa, H., Chen, Y. L., and Israelachvili, J., *J. Phys. Chem.* **97**, 4128–4140 (1993).
[12] Liu, Y., Evans, D. F., Song, Q., and Grainger, D. W., *Langmuir* **12**, 1235–1244 (1996).
[13] Persson, B. N. J., *Phys. Rev. B* **51**, 13568–13585 (1995).
[14] Zilberman, S., Persson, B. N. J., and Nitzan, A., *J. Chem. Phys.* **115**, 11268–11277 (2001).
[15] Chandross, M., Grest, G. S., and Stevens, M. J., *Langmuir* **18**, 8392–8399 (2002).
[16] Georges, J.-M., Tonck, A., and Mazuyer, D., *Wear* **175**, 59–62 (1994).
[17] Kumacheva, E. and Klein, J., *J. Chem. Phys.* **108**, 7010–7022 (1998).
[18] Israelachvili, J. N. and McGuiggan, P. M., *Science* **241**, 795–800 (1988).
[19] Hills, B. A., *Proc. Instn. Mech. Engrs. PtH—J. Engr. Med.* **214**, 83–94 (2000).
[20] Hills, B. A., *Inter. Med. J.* **32**, 242–251 (2002).
[21] Vakarelski, I. U., Brown, S. C., Rabinovich, Y. I., and Moudgil, B. M., *Langmuir* **20**, 1724–1731 (2004).
[22] Grant, L. M. and Tiberg, F., *Biophys. J.* **82**, 1373–1385 (2002).

[23] Drummond, C., Israelachvili, J., and Richetti, P., *Phys. Rev. E* **67**, 066110-1–066110-16 (2003).

[24] Boschkova, K., Feiler, A., Kronberg, B., and Stalgren, J. J. R., *Langmuir* **18**, 7930–7935 (2002).

[25] Roberts, A. D. and Tabor, D., *Proc. R. Soc. Lond. A* **325**, 323–345 (1971).

[26] Richards, S. C. and Roberts, A. D., *J. Phys. D: Appl. Phys.* **25**, A76–A80 (1992).

[27] Klein, J. and Kumacheva, E., *J. Chem. Phys.* **108**, 6996–7009 (1998).

[28] Kumacheva, E., *Prog. Surf. Sci.* **58**, 75–120 (1998).

[29] Briscoe, W. H., Titmuss, S., Tiberg, F., Thomas, R. K., McGillivray, D. J., and Klein, J., *Nature* **444**, 191–194 (2006).

[30] Johnson, K. L., *Contact Mechanics* (Cambridge University Press, London, 2004).

[31] Klein, J., Kumacheva, E., Perahia, D., Mahalu, D., and Warburg, S., *Faraday Discussions*, 173–188 (1994).

[32] Israelachvili, J. N., *Intermolecular and Surface Forces* (Academic Press, London, 1991).

[33] Yamada, S. and Israelachvili, J. N., *J. Phys. Chem. B* **102**, 234–244 (1998).

[34] Burns, A. R., Houston, J. E., Carpick, R. W., and Michalske, T. A., *Phys. Rev. Lett.* **82**, 1181–1184 (1999).

[35] Zielinski, R. and Szymusiak, H., *International J. Quantum Chem.* **99**, 724–734 (2004).

[36] Luzhkov, V. B., Osterberg, F., Acharya, P., Chattopadhyaya, J., and Aqvist, J., *Phys. Chem. Chem. Phys.* **4**, 4640–4647 (2002).

[37] Takekiyo, T. and Yoshimura, Y., *Chem. Phys. Lett.* **420**, 8–11 (2006).

[38] Harmon, K. M., Avci, G. F., and Thiel, A. C., *J. Mol. Struct.* **161**, 205–218 (1987).

[39] Briscoe, W. H. and Horn, R. G., *Langmuir* **18**, 3945–3956 (2002).

[40] Williams-Daryn, S. and Thomas, R. K., *J. Colloid Interface Sci.* **255**, 303–311 (2002).

[41] Neuman, R. D., Park, S., and Shah, P., *J. Phys. Chem.* **98**, 12474–12477 (1994).

[42] Lim, J. C., Neuman, R. D., and Park, S., *Langmuir* **18**, 6125–6132 (2002).

[43] Raviv, U. and Klein, J., *Science* **297**, 1540–1543 (2002).

[44] Raviv, U., Giasson, S., Kampf, N., Gohy, J. F., Jerome, R., and Klein, J., *Nature* **425**, 163–165 (2003).

[45] Stern, H. A. and Feller, S. E., *J. Chem. Phys.* **118**, 3401–3412 (2003).

[46] Teschke, O., Ceotto, G., and de Souza, E. F., *Phys. Chem. Chem. Phys.* **3**, 3761–3768 (2001).

[47] Keren, R. and Shainberg, I., *Clays Clay Minerals* **28**, 204–210 (1980).

[48] Wennerstrom, H., Persson, N., and Lindman, B., *Adv. Chem. Ser.* **9**, 253–269 (1975).

[49] Hamnerius, Y., Lundstrom, I., Paulsson, L. E., Fontell, K., and Wennerstrom, H., *Chem. Phys. Lipids* **22**, 135–140 (1978).

[50] Schniepp, H. C., Saville, D. A., and Aksay, I. A., *J. Am. Chem. Soc.* **128**, 12378–12379 (2006).

[51] Holly, F. J., *Investigative Ophthalmology Visual Sci.* **17**, 552–557 (1978).

[52] Langmuir, I., *Science* **87**, 493–500 (1938).

[53] Rideal, E. and Tadayon, J., *Proc. R. Soc. Lond. A* **225**, 346–356 (1954).

[54] Gaines, G. L. Jr., *Nature* **183**, 1110–1110 (1959).

[55] Gaines, G. L. Jr., *Nature* **186**, 384–385 (1960).

[56] Klein, J., *Proc. Instn. Mech. Engrs. PtH—J. Engr. Med.* **220**, 691–710 (2006).

[57] Bron, A. J., Tiffany, J. M., Gouveia, S. M., Yokoi, N., and Voon, L. W., *Experimental Eye Research* **78**, 347–360 (2004).